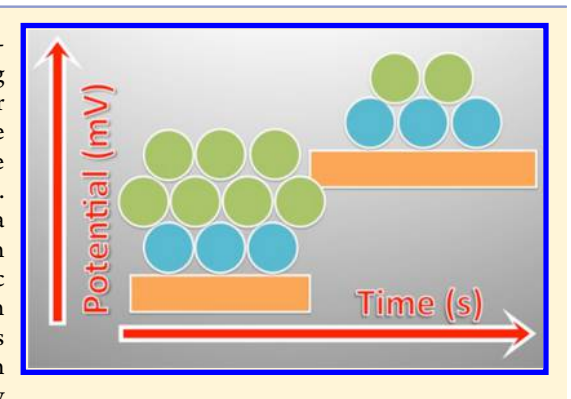


Electrodeposition of In₂Se₃ Using Potential Pulse Atomic Layer Deposition

Justin M. Czerniawski and John L. Stickney*

Department of Chemistry, The University of Georgia, 140 Cedar Street, Athens, Georgia 30602, United States

ABSTRACT: Indium(III) selenide, In₂Se₃, thin films were electrodeposited at room temperature from an aqueous solution containing ionic precursors for both In and Se, using potential pulse atomic layer deposition (PP-ALD). Cyclic voltammetry was used to determine approximate cycle potentials, and anodic and cathodic potentials were systematically examined to optimize the potential pulse program for In₂Se₃. Electron probe microanalysis was used to follow the In:Se atomic ratio as a function of the cycle conditions, and annealing studies were performed on stoichiometric deposits. Film thickness was a function of both the anodic and cathodic potentials. The optimum growth rate was consistent with previous PP-ALD studies in which similar concentrations and pulse times were employed, 0.02 nm/cycle. The use of the potential pulse cycle for film growth resulted in surface-limited control over the deposit stoichiometry each cycle and thus a layer-by-layer growth process.



■ INTRODUCTION

Potential pulse atomic layer deposition (PP-ALD) is an electrodeposition methodology that combines concepts from sequential monolayer deposition (SMD), $^{1-4}$ pulse-reversal deposition (PR), $^{5-8}$ pulsed potentiostatic electrodeposition (PPE), 9 coelectrodeposition 10 (codep), and electrochemical atomic layer deposition (E-ALD) $^{11-20}$ to create E-ALD quality films at increased deposition rates. The advantages of electrodeposition in general are scalability, low cost, low temperature, high energy efficiency, and ease of recycling. A previous PP-ALD study of the growth of Cu_2Se showed a viable thin-film growth method for the binary compound semiconductor. 21

In PP-ALD, potentials are alternated between optimized cathodic and anodic potentials in a cycle, foregoing the use of cyclic voltammetry (CV) or solution alternation required in SMD and E-ALD, respectively. In this version of PP-ALD, the cathodic potential is positioned where both elements deposit near where codep might be performed, but only for a time sufficient to form a fraction of a monolayer (ML). This method qualifies as a form of ALD because it is based on repeated application of a surface-limited reaction to grow deposits an atomic layer at a time. Electrochemical surface-limited reactions are frequently referred to as underpotential deposition (UPD). UPD occurs at a potential that takes advantage of compound formation energetics to selectively form a deposit of one element on another. In this form of PP-ALD, the anodic potential is essentially used to achieve UPD. That is, the anodic potential is used to oxidatively strip any elemental excess and create a stoichiometric deposit surface. During codepeposition, where a single potential or current density is used to control deposit growth, local excesses of an element can result in variations in stoichiometry. By limiting the amount deposited using the time for the cathodic pulse, PP-ALD avoids burying any elemental

excess as it remains accessible to stripping during the anodic pulse. CuInSe $_2$ (CIS) is a highly stable, chalcopyrite semiconductor with potential applications in p-type photovoltaics, light-emitting diodes, optoelectronics, and nonlinear optical devices. ^{19,22–24} CIS has a direct bandgap around 1.08 eV^{22,24} and a high absorption coefficient ($a \sim 10^5 \text{ cm}^{-1}$) leading to laboratory efficiencies as high as 15%. ^{19,23–25} CIS has been formed using techniques such as coevaporation; ²⁶ flash evaporation; ²⁷ chemical vapor deposition; ²⁸ chemical spray pyrolysis; ^{29,30} chemical synthesis; ³¹ selenization of sputtered, ³² evaporated, ²⁶ or electrodeposited ³³ Cu and In stacked layers; ³⁴ electrochemical codeposition; ^{35–37} and pulse electrodeposition. ^{19,22,23,38}

The ternary compound CIS could be manufactured by sequential PP-ALD of binary selenides, such as In_2Se_3 and Cu_2Se . Deposition of Cu_2Se , using PP-ALD, has recently been reported. In₂Se₃ is the subject of the present report. Subsequently, CIS could be formed by alternation of In_2Se_3 and Cu_2Se , followed by annealing.

 $\rm In_2Se_3$ is an n-type semiconductor, with a direct bandgap around 1.62 eV 39 that has potential applications as a two-dimensional material and an absorber layer in photovoltaic devices. 40,41 $\rm In_2Se_3$ has been formed using numerous techniques including chemical bath deposition, 42,43 sputtering, $^{44-46}$ metal organic chemical vapor phase deposition, 47 spray pyrolysis, 48,49 magnetron sputtering, $^{44-46}$ and electrochemical deposition. Photovoltaic (PV) materials have been successfully grown using

Special Issue: Kohei Uosaki Festschrift

Received: January 11, 2016 Revised: February 11, 2016 Published: February 16, 2016



electrodeposition since Kröger et al.'s single-solution, coelectrodeposition (codep), CdTe work in the 1970s. The present report describes an initial investigation into the growth of In_2Se_3 using PP-ALD.

■ EXPERIMENTAL SECTION

The solution was pH 1, 1.5 mM In(ClO₄)₃ (Sigma-Aldrich), 0.1 mM SeO₂ (Alfa Aesar 99.999% pure), and 0.5 M NaClO₄ in 18 M Ω Millipore Advantage 10 water fed by a house deionized water source. The precursor concentrations were kept in the millimolar range to limit deposited amounts to a fraction of a monolayer (ML) each cycle. A ML is defined for this article as one atom for each Au substrate surface atom, or about 1.2×10^{15} atoms per cm². Substrates were 100 nm thick Au films on 5 nm of Ti on glass, purchased from Evaporated Metal Films (Ithaca, NY), and were cleaned by three 5 min sonications in fresh aliquots of acetone, followed by three more of 18 M Ω water. They were then dipped in concentrated nitric acid for 30 s, rinsed with 18 M Ω water, and dried with nitrogen before being placed in the electrochemical flow cell (Figure 1). The cell (Electro-

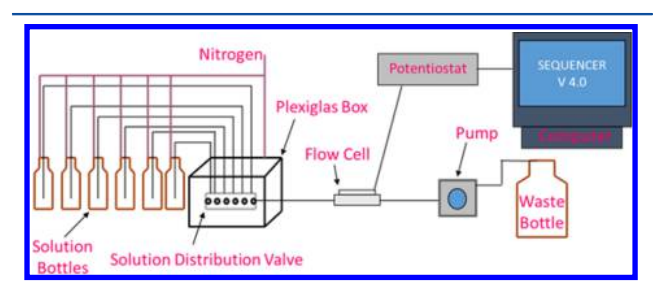


Figure 1. Schematic of the electrochemical flow system. From left to right, solution is drawn from nitrogen-purged solution bottles by a pump through the solution distribution valve, housed in a nitrogen purged Plexiglas box, and "Z" configuration flow cell.

chemical ALD L.C.) was immediately flushed with 0.1 M $\rm H_2SO_4$ (Fisher Scientific, certified ACS plus), and the potential was alternated four times for 5 s at a time between +1400 and -200 mV, completing cleaning of the Au surface. All potentials are reported versus Ag/AgCl.

Figure 1 diagrams the electrochemical flow system, where the auxiliary electrode was an Au wire inlayed into a Plexiglas cell face. A 3 M Ag/AgCl reference electrode (BASi, West Lafayette, IN) was used, and the solution was pulled from degassed solution reservoirs though the cell using a Masterflex (Cole Parmer) peristaltic pump. The system was automated using a program developed in-house named Sequencer.

Electron probe microanalysis (EPMA) was performed on a JEOL 8600 Superprobe instrument with a 10 keV accelerating voltage, 15 nA beam current, and 10 μ m beam diameter. X-ray diffraction was performed on a PANalytical X'PERT Pro instrument with an open Eulerian cradle, utilizing a 1.54 Å Cu K α_1 source and a parallel plate collimator. Spectroscopic ellipsometry was performed on a J.A. Woolam M-200 V instrument.

RESULTS AND DISCUSSION

Figure 2 depicts cyclic voltammetry for Au substrates in separate In (Figure 2a) and Se (Figure 2b) precursor solutions, in the In precursor solution where the substrate was precoated with 0.6 ML of Se (Figure 2c), and in a solution containing precursors for both In and Se (Figure 2d). Figure 2a shows a cyclic voltammogram in $In(ClO_4)_3$ at pH 1, which displays an initial

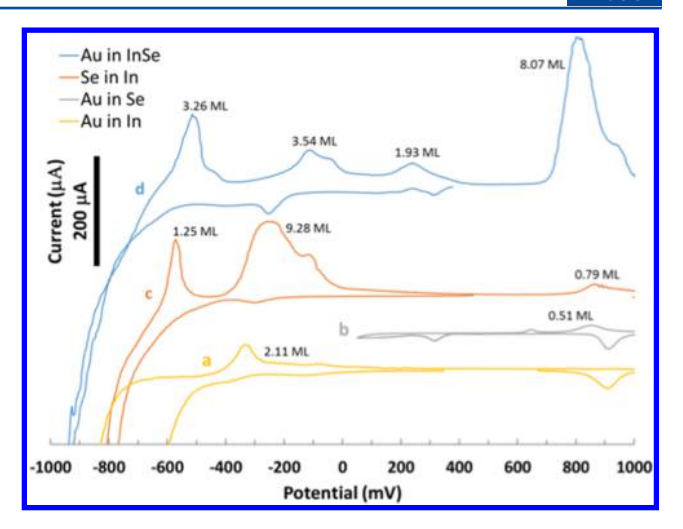


Figure 2. Cyclic voltammogram of (a) Au in 1.5 mM $In(ClO_4)_3$, (b) Au in 0.1 mM SeO_2 , (c) ~0.6 ML Se in 1.5 mM $In(ClO_4)_3$, and (d) Au in 1.5 mM $In(ClO_4)_3$ and 0.1 mM SeO_2 . All solutions were pH 1. Potential was measured versus the Ag/AgCl reference electrode with a scan rate of 10 mV/s. The flow rate was 4 mL/min. The electrode area was 0.79 cm².

scan negative to -1000 mV but is off scale below -600 mV because of the hydrogen evolution reaction (HER). In UPD begins near 100 mV and displays features at -100 and -400 mV, just prior to extensive hydrogen evolution. In the subsequent positive-going scan there is no peak for bulk In stripping, which should occur near -600 mV, the E^{0} for In^{3+} . There is an oxidation peak at -325 mV, which is felt by the authors to be oxidative dissolution of In from a surface alloy with the Au substrate. The peak near -100 mV is In UPD stripping. The deposition of bulk In from the pH 1 solution appeared to be hindered by strong HER, in that a large fraction of the cell was filled with hydrogen bubbles, rather than solution, and it may be that they coated the surface, limiting In³⁺ access. Similar In³⁺ scans in a pH 3 solution shifted the HER negative, allowing the facile deposition of bulk In and the In/Au alloy. The reduction feature at 900 mV is Au oxide reduction.

Figure 2b is a cyclic voltammogram in 0.1 mM HSeO $_3$ ⁻, pH 1. The formal potential is believed to be near 650 mV, suggesting that all Se deposition occurred at an overpotential, consistent with its slow deposition kinetics. S2-54 Surface-limited peaks, related to UPD, are evident at 350 and 200 mV during the negative scan, along with a small amount of bulk Se formation. Stripping of the selenium in the subsequent positive-going scan begins at 650 mV with a small bulk peak and finishes with oxidation of Se in contact with the Au surface at 850 mV.

Figure 2c is also a cyclic voltammogram in $In(ClO_4)_3$, pH 1, to -1000 mV; however, the Au substrate was first coated with 0.6 ML of Se. The reduction feature starting negative of -200 mV appears to be In UPD (Figure 2a). Subsequent reduction below -400 mV includes In reacting with Se on the surface, In/Au alloy formation, bulk In formation, and extensive HER. Comparison of panels a and c in Figure 2, however, indicated that the adsorbed Se increased the hydrogen overpotential, pushing it 150 mV more negative. The reduction peaks below 350 mV for Se deposition (Figure 2b) are not evident in Figure 2c, as the Se was preadsorbed. The first oxidation peak in the positive-going scan, -600 mV, is bulk In stripping, agreeing with the $E^{0'}$. The extensive oxidation feature beginning at -400 mV is consistent with In stripping from the near-surface In/Au alloy. From a comparison of panels a and c in Figure 2, it can be seen that there

is an order of magnitude more In on, or in, the surface when Se was preadsorbed. This is consistent with the hypothesis that HER was interfering with In deposition in Figure 2a, and the adsorbed Se worked to increase the hydrogen overpotential allowing In deposition. The shoulder at -100 mV on the dealloying peak in Figure 2c matches the UPD stripping of In (Figure 2a) while the oxidation peak above 800 mV matches the Se oxidation feature (Figure 2b).

Figure 2d is a cyclic voltammogram in a pH 1 solution containing 1.5 mM In³⁺ and 0.1 mM $HSeO_3^-$, also to -1000 mV. The scan began negative from 400 mV, the open circuit potential (OCP). The first reduction feature, at 325 mV, is similar to the peak in Figure 2b for Se deposition. HSeO₃⁻ reduction may also account for the current between 200 and -100 mV. The reduction peak at -250 mV is consistent with In UPD, though larger, suggesting a reaction between In and Se. The hydrogen overpotential shifted negative, the HER occurring rapidly negative of -700 mV, suggesting its suppression resulted from the surface being coated with a mix of In and Se. During the subsequent positive-going scan the first oxidative feature (-550mV in Figure 2d) is consistent with oxidation of bulk In. Some bulk In was expected, given the 15-fold excess of In to Se in solution. The oxidation peak for In from an In/Au alloy (-250 mV in Figure 2c) is not present. Instead, there is a broad range of oxidation current between -500 and 400 mV (Figure 2d) which appears to be In oxidation from a mixed In/Se layer. The majority of that In was more stable than it was in the In/Au alloy (Figure 2c), suggesting the formation of a compound with Se. The lack of current for In stripping from an In/Au alloy suggests that the formation of a layer of some In/Se compound which blocked diffusion of In into the Au. The large peak above 700 mV in Figure 2d is consistent with bulk Se oxidation, left after oxidative stripping of In. The shoulder at 900 mV corresponds to oxidation of the last layer of Se from the Au substrate.

Figure 3 is a potential time diagram for 5 PP-ALD cycles used in the present study. The cycle begins with 0.13 s at -1000 mV,

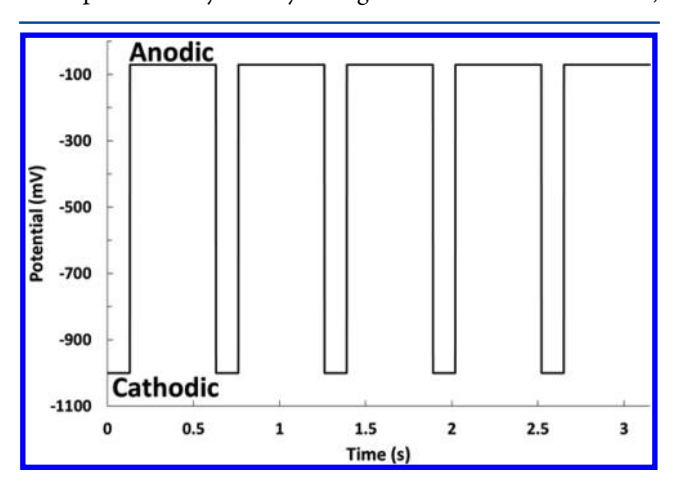


Figure 3. Potential profile for 5 PP-ALD cycles.

the cathodic potential, where fractions of monolayers of Se and In are deposited. The potential is then stepped to $-70 \, \mathrm{mV}$ for 0.5 s, the anodic potential, where any excess In is removed to create the stoichiometric deposit. Figure 4 is a schematic diagram of one PP-ALD cycle.

Two studies were performed to investigate the dependence of the deposit on the anodic and cathodic cycle potentials. Figure 5 displays the deposit thickness of a set of 3300 cycle deposits,

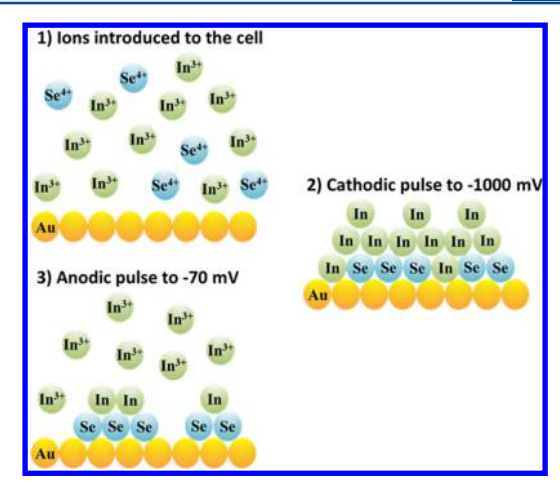


Figure 4. PP-ALD schematic diagram. (1) In^{3+} (green) and Se^{4+} (blue) ions are introduced into the cell at the open circuit potential. (2) The potential is pulsed to $-1000 \,\text{mV}$ for 0.13 s, resulting in the deposition of less than a monolayer of Se and excess In. (3) The potential is then stepped to $-70 \,\text{mV}$ for 0.5 s, removing any excess In from the deposit.

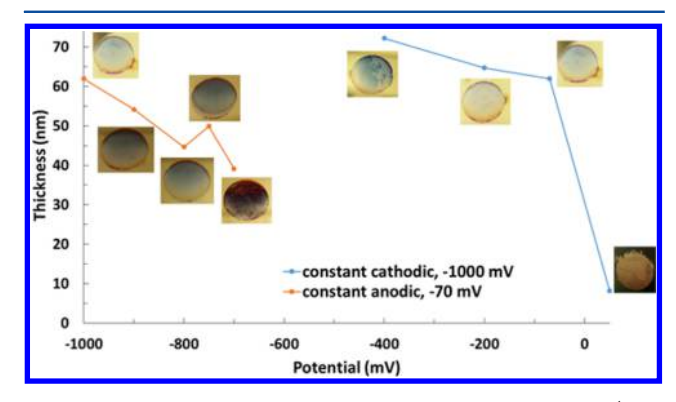


Figure 5. Thickness versus potential under constant cathodic (blue, -1000~mV) and constant anodic (orange, -70~mV) conditions. Each deposit was formed with 3300 pulses.

measured using spectroscopic ellipsometry, where the cathodic potential was held constant (blue) at -1000 mV and the anodic potential was varied. Figure 6 displays the average stoichiometry

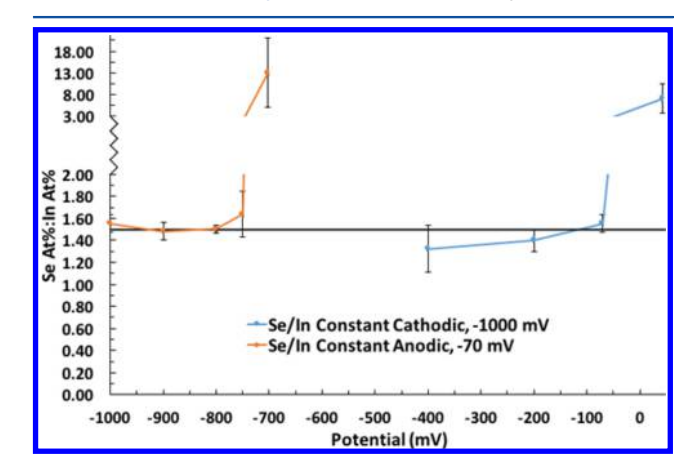


Figure 6. Deposit stoichiometry, determined by EPMA, of Figure 5 deposits made under constant cathodic (blue, -1000 mV) and constant anodic (orange, -70 mV) potentials. The error bars are indicative of homogeneity across the surface. In the blue curve, the anodic potential was varied. In the orange curve, the cathodic potential was varied. Each deposit was formed using 3300 cycles.

(Se/In ratio) and standard deviation (error bars) of 6 points taken across the surface from the set used in Figure 5. The trend was for the thickness to slowly decrease as the anodic potential was increased from -400 to 50 mV. At -400 mV, bulk In should have been removed (Figure 2d); however, from Figure 6 is can be seen that the Se/In ratio was about 1.35 rather than the 1.5 expected for In₂Se₃, indicating that In was in excess. Not removing all excess In at -400 mV is also consistent with a thicker deposit (Figure 5). As the anodic potential was increased, more In was removed and the stoichiometry moved closer to the expected 1.5 (Figure 6). By 50 mV, all In was removed and only Se remained.

From above, an anodic potential of -70 mV was selected as near optimal, and a study varying the cathodic potential was performed (Figure 5, orange). The orange points show that the deposit thickness decreased as the cathodic potential was raised, though the stoichiometry remained 1.5 up to -800 mV (Figure 6, orange). Visible inspection (Figure 5, orange) of deposits formed using a cathodic potential above -1000 mV displayed a gradient in color, white to blue to orange, from ingress to egress (bottom to top), with color being closely related to thickness. White corresponded to thicker areas, while orange deposits were very thin. The near laminar flow in the cell can result in a pattern, thickness gradient, across the deposit when it is at least partially controlled by convective mass transfer. On the other hand, there was little visual variation in thickness (Figure 5) or stoichiometry (error bars Figure 6) when -1000 mV was used as the cathodic potential and -200 or -70 mV was used as the anodic potential. In those cases, deposition was controlled by surface-limited reactions, and the anodic potential functioned as a UPD potential to achieve conformal growth and maintain the deposit stoichiometry using the energetics of compound formation. The growth rate of of the -70 mV anodic deposit was calculated to be 0.02 nm/cycle based on 63 nm divided by 3300 cycles.

The stoichiometry did not change dramatically as the deposition potentials were varied (Figure 6). Deposits formed using a constant anodic potential of -70 mV (orange) and a cathodic potential of -700 mV or above were rich in Se because little In was deposited so close to its formal potential. For deposits formed using -1000 mV for the cathodic potential (Figure 6, blue), using more positive anodic potentials also resulted in Se-rich deposits because more In was oxidatively stripped. All In was stripped above -70 mV.

Figure 7 displays XRD patterns recorded for the Au substrate (gray), an as-deposited In_2Se_3 film, and an In_2Se_3 film after annealing. The two peaks originating from the Au substrate are marked with vertical lines. Under the conditions used in this report, XRD peaks for In_2Se_3 were not observed in the as-deposited samples regardless of amount deposited. However, after annealing for 30 min at 300 °C, a number of diffraction peaks were observed and correlated with hexagonal In_2Se_3 (card: In_2Se_3 hex 00-023-0294). Figure 8 shows corresponding SEM images from the film used in Figure 7, before and after annealing. Feature sizes increased significantly after annealing while the Se/In stoichiometry was not affected, remaining at \sim 1.5. This suggests that the initially amorphous In_2Se_3 atoms had sufficient mobility to crystallize with the 300 °C annealing.

CONCLUSION

 In_2Se_3 films 60 nm thick were formed using PP-ALD. PP-ALD is an electrochemical form of ALD, where the surface-limited reactions are achieved using short cycle times, so that each cycle results in less than a compound ML, and two potentials: a

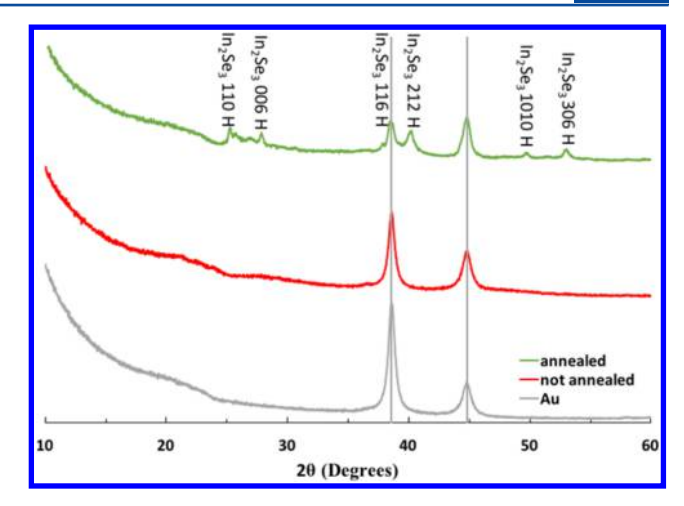


Figure 7. XRD patterns of Au, In_2Se_3 as-deposited, and In_2Se_3 after annealing for 30 min at 300 °C. Cycle potentials were -1000 mV for the cathodic potential and -70 mV for the anodic potential.

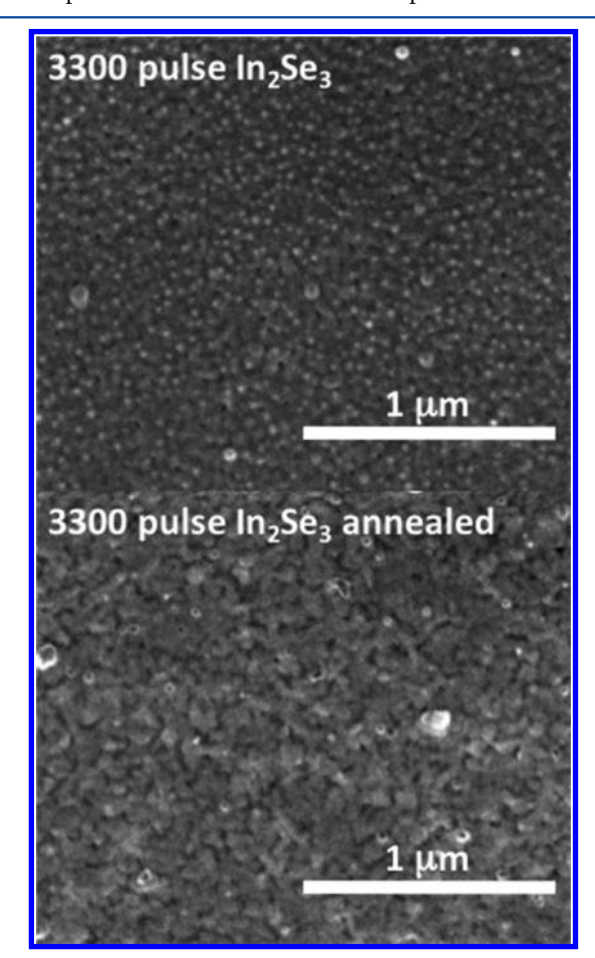


Figure 8. SEM of 3300 cycle In_2Se_3 deposit before and after annealing. Cycle potentials were -1000 mV for the cathodic potential and -70 mV for the anodic potential. The acceleration voltage used was 20.00 kV, and the magnification was a 120 000× objective.

cathodic potential for depositing and an anodic, UPD, potential to achieve conformal growth and a stoichiometric deposit. In this report, the anodic potential was used to remove excess In by oxidative stripping at a potential where the energetics of compound formation controlled the stoichiometry. The advantage of this pulsed form of ALD, relative to previous E-

ALD, is that solutions do not have to be exchanged each cycle; therefore, PP-ALD is faster. In theory, increasing the concentrations by 2 orders of magnitude should increase the rate of deposition by the same. The deposit stoichiometry remained constant over a range of conditions, with a Se:In ratio of 1.5. No XRD pattern was obtained from the as-deposited films, though annealing to 300 °C for 30 min produced a pattern consistent with hexagonal polycrystalline In₂Se₃. The deposition rate was 0.02 nm/cycle under the conditions used here.

AUTHOR INFORMATION

Corresponding Author

*E-mail stickney@uga.edu.

Notes

The authors declare no competing financial interest.

ACKNOWLEDGMENTS

Support from the National Science Foundation, DMR 1410109, is gratefully acknowledged. Thanks are extended to Chris Fleisher and the UGA Microprobe lab. Thanks are extended to the Integrated Bioscience and Nanotechnology Cleanroom for the use of their facilities.

REFERENCES

- (1) Kressin, A. M.; Doan, V. V.; Klein, J. D.; Sailor, M. J. Synthesis of stoichiometric CdSe films via sequential monolayer electrodeposition. *Chem. Mater.* **1991**, *3*, 1015–1020.
- (2) Lee, Y.-C.; Kuo, T.-J.; Hsu, C.-J.; Su, Y.-W.; Chen, C.-C. Fabrication of 3D Macroporous Structures of II–VI and III–V Semiconductors Using Electrochemical Deposition. *Langmuir* **2002**, *18*, 9942–9946.
- (3) Liu, F.; Huang, C.; Lai, Y.; Zhang, Z.; Li, J.; Liu, Y. Preparation of Cu(In,Ga)Se₂ thin films by pulse electrodeposition. *J. Alloys Compd.* **2011**, *509*, L129–L133.
- (4) Ayvazian, T.; van der Veer, W. E.; Xing, W.; Yan, W.; Penner, R. M. Electroluminescent, polycrystalline cadmium selenide nanowire arrays. *ACS Nano* **2013**, *7*, 9469–9479.
- (5) Swaminathan, V.; Murali, K. R. Influence of pulse reversal on the PEC performance of pulse-plated CdSe films. *Sol. Energy Mater. Sol. Cells* **2000**, *63*, 207–216.
- (6) Tang, P. T. Pulse reversal plating of nickel and nickel alloys for microgalvanics. *Electrochim. Acta* **2001**, *47*, 61–66.
- (7) Chandrasekar, M. S.; Pushpavanam, M. Pulse and pulse reverse plating—Conceptual, advantages and applications. *Electrochim. Acta* **2008**, *53*, 3313–3322.
- (8) Lin, J. Y.; Tsai, Y. T.; Tai, S. Y.; Lin, Y. T.; Wan, C. C.; Tung, Y. L.; Wu, Y. S. Pulse-Reversal Deposition of Cobalt Sulfide Thin Film as a Counter Electrode for Dye-Sensitized Solar Cells. *J. Electrochem. Soc.* **2013**, *160*, D46–D52.
- (9) Banga, D.; Lensch-Falk, J. L.; Medlin, D. L.; Stavila, V.; Yang, N. Y. C.; Robinson, D. B.; Sharma, P. A. Periodic Modulation of Sb Stoichiometry in Bi₂Te₃/Bi_{2-x}Sb_xTe₃Multilayers Using Pulsed Electrodeposition. *Cryst. Growth Des.* **2012**, *12*, 1347–1353.
- (10) Massaccesi, S.; Sanchez, S.; Vedel, J. Electrodeposition of indium selenide In₂Se₃. *J. Electroanal. Chem.* **1996**, 412, 95–101.
- (11) Kolb, D. M. Physical and Electrochemical Properties of Metal Monolayers on Metallic Substrates. *Advances in Electrochemistry and Electrochemical Engineering*; Gerischer, H.; Tobias, C. W., Eds.; John Wiley: New York, 1978; Vol. 11, p 125.
- (12) Juttner, K.; Lorenz, W. J. Underpotential Metal Deposition on Single Crystal Surfaces. Z. Phys. Chem. 1980, 122, 163–185.
- (13) Adzic, R. R. Electrocatalytic Properties of the Surfaces Modified by Foreign Metal Ad Atoms. *Advances in Electrochemistry and Electrochemical Engineering*; Gerishcher, H., Tobias, C. W., Eds.; Wiley-Interscience: New York, 1984; Vol. 13, p159.

- (14) Suggs, D. W.; Villegas, I.; Gregory, B. W.; Stickney, J. L. Formation of CdTe and GaAs by electrochemical atomic layer epitaxy (ECALE). MRS Online Proc. Libr. 1991, 222, 283.
- (15) Colletti, L. P.; Stickney, J. L. II-VI compound semiconductor thinfilm electrodeposition by ECALE. *Book of Abstracts*, 210th ACS National Meeting, Chicago, IL, August 20–24, 1995; American Chemical Society: Washington, DC, 1995; INOR-297.
- (16) Colletti, L. P.; Flowers, B. H.; Stickney, J. L. Formation of Thin-Films of CdTe, CdSe, and CdS by Electrochemical ALE. *J. Electrochem. Soc.* 1998, 145, 1442.
- (17) Colletti, L. P.; Slaughter, R.; Stickney, J. L. ZnS thin film formation by electrochemical ALE: preliminary doping studies. *Proceedings of the Symposium on Photoelectrochemistry*; The Electrochemical Society: Pennington, NJ, 1997; 97, 1–10.
- (18) Gewirth, A. A.; Niece, B. K. Electrochemical applications of in situ scanning probe microscopy. *Chem. Rev.* **1997**, *97*, 1129–1162.
- (19) Banga, D.; Jarayaju, N.; Sheridan, L.; Kim, Y. G.; Perdue, B.; Zhang, X.; Zhang, Q.; Stickney, J. Electrodeposition of CuInSe₂ (CIS) via electrochemical atomic layer deposition (E-ALD). *Langmuir* **2012**, 28, 3024–3031.
- (20) Perdue, B.; Czerniawski, J.; Anthony, J.; Stickney, J. Optimization of Te Solution Chemistry in the Electrochemical Atomic Layer Deposition Growth of CdTe. *J. Electrochem. Soc.* **2014**, *161*, D3087–D3092.
- (21) Czerniawski, J. M.; Perdue, B. R.; Stickney, J. L. Potential Pulse Atomic Layer Deposition of Cu₂Se. *Chem. Mater.* **2016**, 28, 583.
- (22) Hu, S.-Y.; Lee, W.-H.; Chang, S.-C.; Cheng, Y.-L.; Wang, Y.-L. Pulsed Electrodeposition of CuInSe₂ Thin Films onto Mo-Glass Substrates. *I. Electrochem. Soc.* **2011**, *158*, B557–B561.
- (23) Caballero-Briones, F.; Palacios-Padrós, A.; Sanz, F. CuInSe₂ films prepared by three step pulsed electrodeposition. Deposition mechanisms, optical and photoelectrochemical studies. *Electrochim. Acta* **2011**, *56*, 9556–9567.
- (24) Hamrouni, S.; AlKhalifah, M. S.; Boujmil, M. F.; Saad, K. B. Preparation and characterization of CuInSe₂ electrodeposited thin films annealed in vacuum. *Appl. Surf. Sci.* **2014**, 292, 231–236.
- (25) Fangyang, L.; Ying, L.; Zhian, Z.; Yanqing, L.; Jie, L.; Yexiang, L. Preparation of Chalcopyrite CuInSe₂ Thin Films by Pulse-Plating Electrodeposition and Annealing Treatment. *Proceedings of ISES World Congress 2007 (Vol. I Vol. V)*; Goswami, D. Y., Zhao, Y., Eds.; Springer: Berlin Heidelberg, 2009; pp 1316–1320.
- (26) Guillén, C.; Herrero, J. Structure, morphology and photoelectrochemical activity of CuInSe₂ thin films as determined by the characteristics of evaporated metallic precursors. *Sol. Energy Mater. Sol. Cells* **2002**, 73, 141–149.
- (27) Ashida, A.; Hachiuma, Y.; Yamamoto, N.; Ito, T.; Cho, Y. CuInSe₂ thin films prepared by quasi-flash evaporation of In₂Se₃ and Cu₂Se. *J. Mater. Sci. Lett.* **1994**, *13*, 1181–1184.
- (28) Jones, P. A.; Jackson, A. D.; Lickiss, P. D.; Pilkington, R. D.; Tomlinson, R. D. The plasma enhanced chemical vapour deposition of CuInSe₂. *Thin Solid Films* **1994**, 238, 4–7.
- (29) Shirakata, S.; Murakami, T.; Kariya, T.; Isomura, S. Preparation of CuInSe₂ Thin Films by Chemical Spray Pyrolysis. *Jpn. J. Appl. Phys., Part* 1 1996, 35, 191–199.
- (30) Terasako, T.; Shirakata, S.; Isomura, S. Photoacoustic Spectra of CuInSe₂ Thin Films Prepared by Chemical Spray Pyrolysis. *Jpn. J. Appl. Phys., Part 1* **1999**, *38*, 4656–4660.
- (31) de Kergommeaux, A.; Fiore, A.; Bruyant, N.; Chandezon, F.; Reiss, P.; Pron, A.; de Bettignies, R.; Faure-Vincent, J. Synthesis of colloidal CuInSe₂ nanocrystals films for photovoltaic applications. *Sol. Energy Mater. Sol. Cells* **2011**, *95*, S39–S43.
- (32) Guillén, C.; Martínez, M. A.; Herrero, J. CuInSe2 thin films obtained by a novel electrodeposition and sputtering combined method. *Vacuum* **2000**, *58*, 594–601.
- (33) Guillèn, C.; Herrero, J. Improved Selenization Procedure to Obtain CulnSe₂ Thin Films from Sequentially Electrodeposited Precursors. *J. Electrochem. Soc.* **1996**, *143*, 493–498.

- (34) Liang, D.; Unveroglu, B.; Zangari, G. Electrodeposition of Cu-In Alloys as Precursors of Chalcopyrite Absorber Layers. *J. Electrochem. Soc.* **2014**, *161*, D613–D619.
- (35) Bhattacharya, R. N. Solution Growth and Electrodeposited CuInSe, Thin Films. *J. Electrochem. Soc.* **1983**, *130*, 2040–2042.
- (36) Kaupmees, L.; Altosaar, M.; Volubujeva, O.; Mellikov, E. Study of composition reproducibility of electrochemically co-deposited CuInSe₂ films onto ITO. *Thin Solid Films* **2007**, *515*, 5891–5894.
- (37) Hernandez-Pagan, E. A.; Wang, W.; Mallouk, T. E. Template electrodeposition of single-phase p- and n-type copper indium diselenide (CuInSe₂) nanowire arrays. ACS Nano 2011, 5, 3237–3241.
- (38) Palacios-Padrós, A.; Caballero-Briones, F.; Sanz, F. Enhancement in as-grown CuInSe₂ film microstructure by a three potential pulsed electrodeposition method. *Electrochem. Commun.* **2010**, *12*, 1025–1029.
- (39) Qasrawi, A. F. Temperature dependence of the band gap, refractive index and single-oscillator parameters of amorphous indium selenide thin films. *Opt. Mater.* **2007**, *29*, 1751–1755.
- (40) Ikari, T.; Shigetomi, S.; Hashimoto, K. Crystal Structure and Raman Spectra of InSe. *Phys. Status Solidi B* **1982**, *111*, 477–481.
- (41) Yadav, A. A.; Salunke, S. D. Photoelectrochemical properties of In₂Se₃ thin films: Effect of substrate temperature. *J. Alloys Compd.* **2015**, 640, 534–539.
- (42) Pathan, H. M.; Kulkarni, S. S.; Mane, R. S.; Lokhande, C. D. Preparation and characterization of indium selenide thin films from a chemical route. *Mater. Chem. Phys.* **2005**, *93*, 16–20.
- (43) Asabe, M. R.; Chate, P. A.; Delekar, S. D.; Garadkar, K. M.; Mulla, I. S.; Hankare, P. P. Synthesis, characterization of chemically deposited indium selenide thin films at room temperature. *J. Phys. Chem. Solids* **2008**, *69*, 249–254.
- (44) Li, S.; Yan, Y.; Zhang, Y.; Ou, Y.; Ji, Y.; Liu, L.; Yan, C.; Zhao, Y.; Yu, Z. Monophase γ-In₂Se₃ thin film deposited by magnetron radio-frequency sputtering. *Vacuum* **2014**, *99*, 228–232.
- (45) Yan, Y.; Li, S.; Yu, Z.; Liu, L.; Yan, C.; Zhang, Y.; Zhao, Y. Influence of indium concentration on the structural and optoelectronic properties of indium selenide thin films. *Opt. Mater.* **2014**, *38*, 217–222.
- (46) Yan, Y.; Li, S.; Ou, Y.; Ji, Y.; Liu, L.; Yan, C.; Zhang, Y.; Yu, Z.; Zhao, Y. In-situ annealing of In—Se amorphous precursors sputtered at low temperature. *J. Alloys Compd.* **2014**, *614*, 368—372.
- (47) Choi, H.; Nicolaescu, R.; Paek, S.; Ko, J.; Kamat, P. V. Supersensitization of CdS quantum dots with a near-infrared organic dye: toward the design of panchromatic hybrid-sensitized solar cells. *ACS Nano* **2011**, *5*, 9238–9245.
- (48) Aydin, E.; Sankir, M.; Sankir, N. D. Influence of silver incorporation on the structural, optical and electrical properties of spray pyrolyzed indium sulfide thin films. *J. Alloys Compd.* **2014**, *603*, 119–124.
- (49) Reyes-Figueroa, P.; Painchaud, T.; Lepetit, T.; Harel, S.; Arzel, L.; Yi, J.; Barreau, N.; Velumani, S. Structural properties of In₂Se₃ precursor layers deposited by spray pyrolysis and physical vapor deposition for CuInSe₂ thin-film solar cell applications. *Thin Solid Films* **2015**, 587, 112
- (50) Kröger, F. A. Cathodic Deposition and Characterization of Metallic or Semiconducting Binary Alloys or Compounds. *J. Electrochem. Soc.* **1978**, *125*, 2028–2034.
- (51) Panicker, M. P. R.; Knaster, M.; Kroger, F. A. Cathodic Deposition Of CdTe From Aqueous-Electrolytes. *J. Electrochem. Soc.* 1978, 125, 566–572.
- (52) Lister, T. E.; Huang, B. M.; Herrick, R. D.; Stickney, J. L. Electrochemical Formation of Se Atomic Layers On Au(100). *J. Vac. Sci. Technol., B: Microelectron. Process. Phenom.* 1995, 13, 1268.
- (53) Lister, T. E.; Stickney, J. L. Atomic level studies of selenium electrodeposition on gold (111) and gold (110). *J. Phys. Chem.* **1996**, 100, 19568–19576.
- (\$4) Huang, B. M.; Lister, T. E.; Stickney, J. L. Se adlattices formed on Au (100), studies by LEED, AES, STM and electrochemistry. *Surf. Sci.* **1997**, 392, 27–43.